Proceedings of the CERN-BINP Workshop for Young Scientists in e^+e^- Colliders, Geneva, Switzerland, 22 – 25 August 2016, edited by V. Brancolini ans L. Linssen, CERN Proceedings, Vol. 1/2017, CERN-Proceedings-2017-001 (CERN, Geneva, 2017)

Calorimetry at the CMD-3 detector

G. P. Razuvaev*[1, 2], R. R. Akhmetshin[1, 2], A. V. Anisenkov[1, 2], V. M. Aulchenko[1, 2], N. S. Bashtavoy[1, 2], D. A. Epifanov[1, 1], L. B. Epshteyn[1, 2, 3], A. L. Erofeev[1, 2], A. A. Grebenuk[1, 2], D. N. Grigoriev[1, 2, 3], V. F. Kazanin[1, 2], O. A. Kovalenko[1, 2], A. N. Kozyrev[1, 2, 3], A. E. Kuzmenko[1, 2], A. S. Kuzmin[1, 2], I. B. Logashenko[1, 2], K. Yu. Mikhailov[1, 2], V. S. Okhapkin[1], A. A. Ruban[1], V. E. Shebalin[1, 2], B. A. Shwartz[1, 2], V. M. Titov[1], A. A. Talyshev[1, 2], and Yu. V. Yudin[1, 2]

[1]Budker Institute of Nuclear Physics, SB RAS, Novosibirsk, 630090, Russia
[2]Novosibirsk State University, Novosibirsk, 630090, Russia
[3]Novosibirsk State Technical University, Novosibirsk, 630092, Russia

Abstract

The general purpose detector CMD-3 has been collecting data since 2010 in an energy range 0.32–2 GeV at the e^+e^- collider VEPP-2000 at the Budeker Institute of Nuclear Physics. The detector physics program includes the study of the e^+e^- annihilation into hadrons. To supply high registration efficiency for neutral particles the CMD-3 has an electromagnetic calorimeter consisting of three subsystems: BGO endcap calorimeter and barrel with an inner part based on LXe and an outer one based on CsI crystals. The main parameters of calorimeters, cluster reconstruction and calibration procedures with performance results are described.

Keywords

Calorimetry; liquid xenon; scintillation crystals.

1 Introduction

The VEPP-2000 [1, 2] is an e^+e^- collider at the Budker Institute of Nuclear Physics (Novosibirsk, Russia). It operates in a center-of-mass (c. m.) energy range from 0.32 to 2 GeV. The designed luminosity of the collider at 2 GeV c. m. energy is 10^{32} cm^{-2} s^{-1}. In order to reach the design luminosity in a single-bunch mode the novel round beam technique developed at the BINP is used. The beam energy is monitored with a precision of $\Delta E/E = 6 \cdot 10^{-5}$ using the Compton backscattering process [3, 4]. There are two interaction points at the collider and two detectors are mounted there: the Spherical Neutral Detector (SND) [5, 6] and the Cryogenic Magnetic Detector (CMD-3) [7]. Data taking started in 2010. The integrated luminosity collected by each detector during three years of operation is about 60 pb^{-1}. In 2013 the collider operation was stopped for a collider and detectors upgrade, and it has been resumed in 2017.

The physical program [8, 9, 10] includes measurement of the $e^+e^- \to hadrons$ cross sections, study of the properties of known and search for new vector mesons, measurement of $n\bar{n}$ and $p\bar{p}$ cross sections near their thresholds and search for exotic hadrons. These tasks require a detector with high efficiency for multiparticle events and good energy and angular resolutions for both charged particles and photons.

The CMD-3 is a general purpose detector. Its layout is presented in Figure 1. The electromagnetic calorimeter is one of the most important systems of the CMD-3 detector. Its main goals are measurements of energy and coordinate of the photons, the separation of electrons from hadrons and a generation of signals for the neutral trigger. The calorimetry of the detector consists of barrel and endcap parts. The

*G.P.Razuvaev@inp.nsk.su

https://doi.org/10.23727/CERN-Proceedings-2017-001.71

barrel calorimeter combines the inner liquid xenon calorimeter (LXe) [11] and the outer one based on CsI crystals [12]. The endcap calorimeter [13] is based on the bismuth germanium oxide $Bi_4Ge_3O_{12}$ (BGO) crystals. The total solid angle coverage of the CMD-3 calorimeter is equal to $0.94 \times 4\pi$.

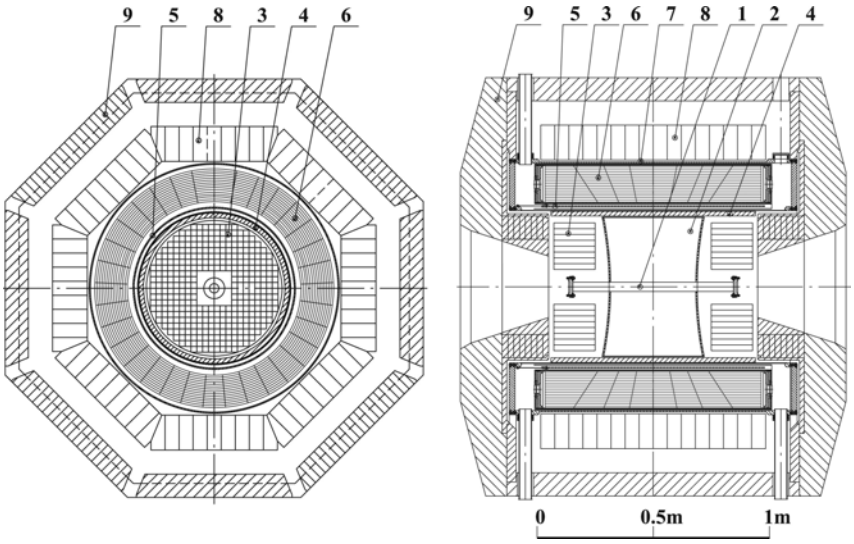

Fig. 1: The CMD-3 detector layout: 1 — beam pipe, 2 — drift chamber, 3 — BGO endcap calorimeter, 4 — Z-chamber, 5 — superconducting solenoid, 6 — liquid xenon calorimeter, 7 — time-of-flight system, 8 — CsI calorimeter, 9 — yoke

2 General description

The inner LXe calorimeter is a set of 14 ionization chambers with 7 cylindrical cathodes and 8 anodes divided by 10.2 mm gaps between them. The calorimeter is placed in the same vacuum vessel with a superconducting solenoid to reduce passive material in front of the calorimeter. The electrodes are made of a 0.5 mm thin G-10 plate foiled with copper. The conductive surfaces of the anode cylinders are divided into 264 rectangular pads (8 along the Z-axis and 33 in the $r - \phi$ plane) forming so-called "towers" oriented to the beam interaction point. Pads within one tower are electrically connected. The average tower size is $8 \times 10 \times 15$ cm^3. The signals from the towers are used to measure the deposited energy. The cathode cylinders are divided into 2112 strips to provide a precise coordinate measurement together with the measurement of specific energy losses. Each side of the cathode cylinder contains about 150 strips. The strips on the opposite sides of the cylinder are mutually perpendicular. One signal strip consists of four joined 2 mm width strips. Such semi-transparent electrode structures provide charge induction on both sides of cathode electrode. That allows one to determine both coordinates of the photon conversion point using the information from one gap only. The design of the liquid xenon calorimeter is described in detail in [14, 11].

Since the LXe calorimeter is rather thin (5.4 X_0) it is surrounded by the CsI scintillation crystals calorimeter to improve the energy resolution. The CsI calorimeter consists of 1152 $6 \times 6 \times 15$ cm^3 Na- or Tl-doped CsI crystals assembled in 8 octants. Each octant consists of 9 rows (modules) of crystals. The modules are oriented along the Z-axis. Both sides of the modules of each octant have a special truncated shape in order to avoid gaps between octants. Each module consists of 16 counters. The length of the crystals corresponds to a thickness of 8.1 X_0. The total sensitive material thickness of the barrel calorimeter for a normal incident particle is equal to 13.5 X_0. The thickness of the passive material in front of the barrel calorimeter is 0.35 X_0 and passive material between LXe and CsI parts of the barrel calorimeter is 0.25 X_0. The design of the CsI calorimeter is described in detail in [12].

To increase the solid angle coverage the CMD-3 is equipped with the endcap calorimeter. It consists of 680 BGO crystals of $2.5 \times 2.5 \times 15$ cm^3 arranged in two identical arrays. The endcap calorimeters cover polar angles from 17° to 50° and from 130° to 163°. The length of the crystals corresponds to the thickness of 13.4 X_0. The design of this calorimeter is described in detail in [15].

3 Cluster reconstruction

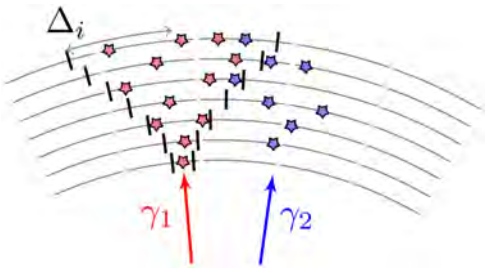

Fig. 2: Cluster reconstruction in the LXe calorimeter from strip information

The standard cluster reconstruction procedure in crystal and LXe calorimeters begins with searching for a calorimeter element with energy deposition, greater than 5 MeV, a seed. Then all neighbour elements having at least 2 MeV of energy deposition are grouped together in one cluster and the procedure is repeated. This algorithm introduces a limitation on the minimal distance between clusters in the LXe calorimeter to be properly reconstructed. The distance equals a tower size corresponding to ~ 40 mrad. This is not sufficient for multiparticle processes and for high energy π^0 decaying into two photons. Because of that the development of the new reconstruction algorithm [16] has been started to separate close incident photons based on LXe strip information. Firstly, using simulation the most probable radius Δ_i of an electromagnetic shower for each cathode layer was determined. Then for a tower cluster the conversion point — closest to the interaction point cross-section of strip clusters — is treated as a seed to which the connection of strip clusters with respect of Δ_i is performed, see Figure 2. Groups of leftover strips in the tower cluster are considered as another photon. At the next step sorting of strip photons by energy calculated from strip information is done and the top two energetic photons are saved, the others are rejected. In the end one has precise knowledge about the photons' conversion points and their combined energy measured with the anode structure and rough energy estimation of each photon by cathode signals. A test of the new algorithm was done with simulation data of the $e^+e^- \to \pi^0\gamma$ process for energies from 1 GeV to 2 GeV in the centre of mass frame. The result shows a significant growth in the detection efficiency for high energies.

4 Calibrations and resolutions

Several procedures are used for the calorimeter calibration. Electronic channel calibration with a pulse generator provides the measurement of the pedestals, electronic gain and electronic noise of each calorimeter channel. For crystal calorimeters cosmic ray particles in special calibration runs are used. Since the standard CMD-3 trigger does not suppress all cosmic rays events the experimental data sample contains such events and they are also used for the calibration. This type of calibration is used for both endcap and combined barrel calorimeters. For LXe calorimeter a calibration with e^+e^- elastic scattering events is used. For the endcap calorimeter the energy corrections are performed using the two-photon annihilation process, $e^+e^- \to \gamma\gamma$, to obtain absolute energy calibration. The calibration procedures for the joined barrel calorimeter are described in [17] and for the endcap calorimeter in [13].

Two-photon annihilation and Bhabha events were used to obtain the energy and spatial resolutions of the calorimeters. The results are shown in Figure 3 and Figure 4.The problems in the

calorimeter electronics in 2010–2013 caused the rise of LXe+CsI σ_E/E for high beam energies in Figure 3. The electronics were fixed during the collider shutdown. The energy resolution for the barrel calorimeter can be parametrized as $\sigma_E/E = 0.034/\sqrt{E/\text{GeV}} \oplus 0.020$ and for the endcap as $\sigma_E/E = 0.024/\sqrt{E/\text{GeV}} \oplus 0.023$.

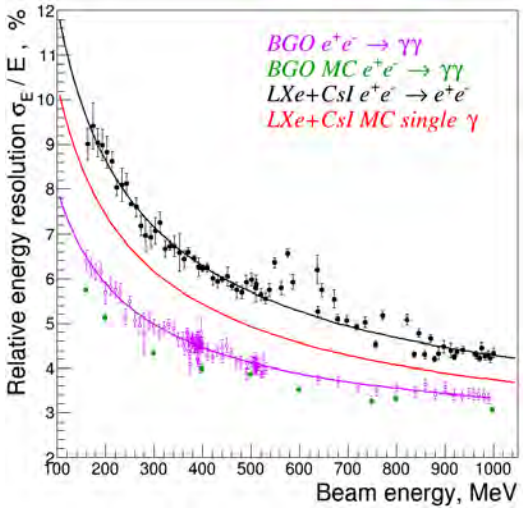

Fig. 3: Energy resolution of calorimeters

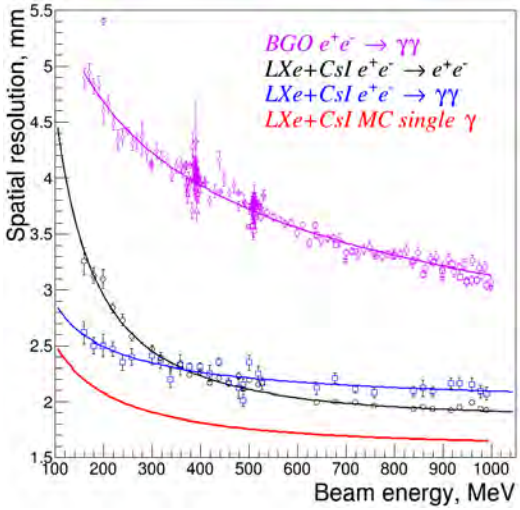

Fig. 4: Spatial resolution of calorimeters

To obtain the spatial resolution of the calorimeters the distribution of the azimuth angle acollinearity $\Delta\phi = \pi - |\phi_1 - \phi_2|$ was used, where ϕ_1 and ϕ_2 are the azimuth angles of the photons. This distribution was approximated by a Gaussian function, the angular resolution of the calorimeter σ_ϕ was defined as the standard deviation of the Gaussian function. The coordinates of most (95%) photons detected in the barrel calorimeter are measured using LXe strips data with an angular precision of about 0.005 rad, which slightly depends on the photon energy. In this case the angular resolution can be fitted as $\sigma_\varphi/\text{mrad} = 3.70 + 0.33/(0.25 + E/\text{GeV})$. For about 5% of events the conversion point is not reconstructed by strip data and the photon coordinates are determined as the centre of gravity of the cluster. For such a case the correction function for the photon coordinates was determined from the simulation. The angular resolution in this case can be fitted as $\sigma_\varphi/\text{mrad} = 37.0 + 3.6/(0.1 + E/\text{GeV})$.

The spatial resolution of the endcap calorimeter was calculated as $\sigma_x = \sigma_\varphi \cdot Z_0 \cdot \tan\theta/\sqrt{2}$ where Z_0 is the distance from the interaction point to the front plane of the endcap and θ is the polar angle of the photon. The resolution can be fitted as $\sigma_x/\text{mm} = 3.03/\sqrt[4]{E/\text{GeV}}$.

Finally, to demonstrate the calorimetry performance Fig. 5 and Fig. 6 contain the distribution of photon invariant masses obtained during analyses of $e^+e^- \to \pi^+\pi^-\pi^0$ and $e^+e^- \to \pi^0\gamma$, $\eta\gamma$ with pseudo-scalars decaying into two photons. For the first process the π^0 mass resolution is about 8.5% and 5.8% for η-meson in the second process.

5 Conclusion

The calorimeters were installed into the CMD-3 detector and have been used in the experimental data taking since 2010. The calibration procedures of the calorimeters have been developed and used during all three physics seasons. The standard photon energy reconstruction procedures have been developed and applied, the new algorithm using strip information to separate close photons is under design. The energy and spatial resolutions at 1 GeV have been determined to be 4.5% and 2 mm for the barrel calorimeter and 3.5% and 3 mm for the endcap calorimeter respectively.

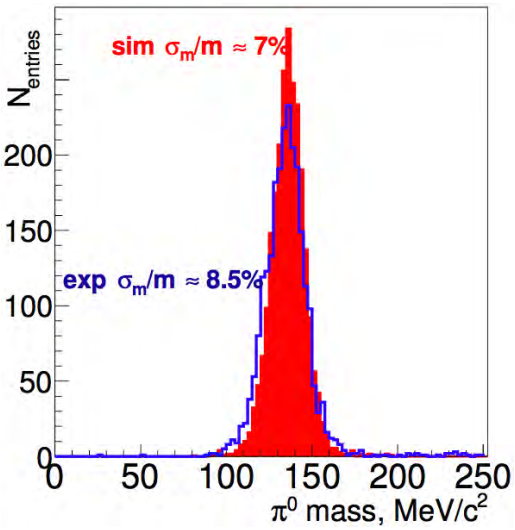

Fig. 5: The distribution of the two photon invariant mass in the $e^+e^- \to \pi^+\pi^-\pi^0$ process before kinematic reconstruction. The comparison of experimental (open blue) and simulation (closed red) data is presented.

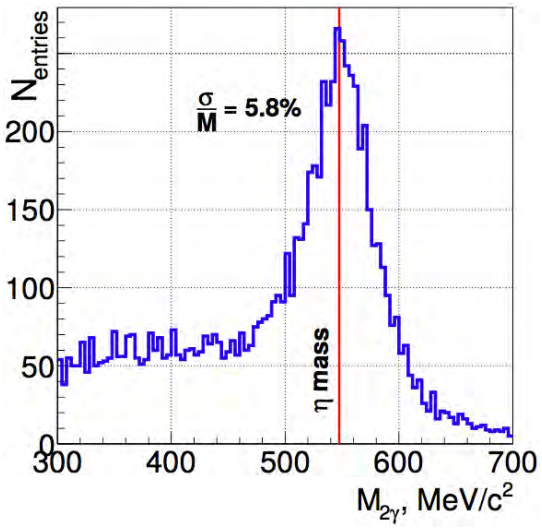

Fig. 6: The distribution of the two photon invariant mass in the $e^+e^- \to 3\gamma$ process before kinematic reconstruction. The signal peak shown from $e^+e^- \to \eta\gamma$.

Acknowledgements

This work has been supported by Russian Science Foundation (project N 14-50-00080).

References

[1] Yu. M. Shatunov et al. “Project of a new electron positron collider VEPP-2000”. In: *Conf. Proc.* C0006262 (2000). [,439(2000)], pp. 439–441 (cit. on p. 1).

[2] D. Berkaev et al. “VEPP-2000 operation with round beams in the energy range from 1-GeV to 2-GeV”. In: *Nucl. Phys. Proc. Suppl.* 225-227 (2012), pp. 303–308. DOI: 10.1016/j.nuclphysbps.2012.02.063 (cit. on p. 1).

[3] E. V. Abakumova et al. “A system of beam energy measurement based on the Compton backscattered laser photons for the VEPP-2000 electron–positron collider”. In: *Nucl. Instrum. Meth.* A744 (2014), pp. 35–40. DOI: 10.1016/j.nima.2014.01.020. arXiv: 1310.7764 [physics.acc-ph] (cit. on p. 1).

[4] E. V. Abakumova, M. N. Achasov, A. A. Krasnov, et al. “The system for delivery of IR laser radiaton into high vacuum”. In: *JINST* 10.09 (2015), T09001. DOI: 10.1088/1748-0221/10/09/T09001. arXiv: 1504.00130 [physics.acc-ph] (cit. on p. 1).

[5] M. N. Achasov et al. “First experience with SND calorimeter at VEPP-2000 collider”. In: *Nucl. Instrum. Meth.* A598 (2009), pp. 31–32. DOI: 10.1016/j.nima.2008.08.012 (cit. on p. 1).

[6] M. N. Achasov et al. “Time resolution of the SND electromagnetic calorimeter”. In: *JINST* 10.06 (2015), T06002. DOI: 10.1088/1748-0221/10/06/T06002 (cit. on p. 1).

[7] B. Khazin. “Physics and detectors for VEPP-2000”. In: *Nucl. Phys. Proc. Suppl.* 181-182 (2008), pp. 376–380. DOI: 10.1016/j.nuclphysbps.2008.09.068 (cit. on p. 1).

[8] S. Eidelman. “Physics at VEPP-2000”. In: *Nucl. Phys. Proc. Suppl.* 162 (2006). [,323(2006)], pp. 323–326. DOI: 10.1016/j.nuclphysbps.2006.09.122 (cit. on p. 1).

[9] R. R. Akhmetshin et al. "Search for the process $e^+e^- \to \eta'(958)$ with the CMD-3 detector". In: *Phys. Lett.* B740 (2015), pp. 273–277. DOI: 10.1016/j.physletb.2014.11.056. arXiv: 1409.1664 [hep-ex] (cit. on p. 1).

[10] D. N. Shemyakin et al. "Measurement of the $e^+e^- \to K^+K^-\pi^+\pi^-$ cross section with the CMD-3 detector at the VEPP-2000 collider". In: *Phys. Lett.* B756 (2016), pp. 153–160. DOI: 10.1016/j.physletb.2016.02.072. arXiv: 1510.00654 [hep-ex] (cit. on p. 1).

[11] A. V. Anisenkov et al. "Status of the Liquid Xenon calorimeter of the CMD-3 detector". In: *JINST* 9 (2014), p. C08024. DOI: 10.1088/1748-0221/9/08/C08024 (cit. on p. 2).

[12] V. M. Aulchenko et al. "CsI calorimeter of the CMD-3 detector". In: *JINST* 10.10 (2015), P10006. DOI: 10.1088/1748-0221/10/10/P10006 (cit. on p. 2).

[13] R. R. Akhmetshin, D. N. Grigoriev, V. F. Kazanin, et al. "Performance of the BGO endcap calorimeter of the CMD-3 detector". In: *JINST* 9.10 (2014), p. C10002. DOI: 10.1088/1748-0221/9/10/C10002 (cit. on pp. 2, 3).

[14] A. V. Anisyonkov, L. M. Barkov, N. S. Bashtovoy, et al. "Liquid xenon calorimeter for a CMD-3 detector". In: *Nucl. Instrum. Meth.* A598 (2009), pp. 266–267. DOI: 10.1016/j.nima.2008.08.091 (cit. on p. 2).

[15] R. R. Akhmetshin, D. N. Grigoriev, V. F. Kazanin, et al. "Status of the endcap BGO calorimeter of the CMD-3 detector". In: *Physics of Atomic Nuclei* 72.3 (2009), pp. 477–481. DOI: 10.1134/S1063778809030119 (cit. on p. 3).

[16] Andrey Rabusov. "The study of the annihilation process $e^+e^- \to \eta\gamma$, $\eta \to \pi^+\pi^-\pi^0$ with the CMD-3 detector at the VEPP-2000 collider". MA thesis. Novosibirsk, Russia: Novosibirsk State University, June 2016 (cit. on p. 3).

[17] V. E. Shebalin et al. "Combined Liquid Xenon and crystal CsI calorimeter of the CMD-3 detector". In: *JINST* 9.10 (2014), p. C10013. DOI: 10.1088/1748-0221/9/10/C10013 (cit. on p. 3).